Annals of Nuclear Medicine Vol. 8, No. 2, 101–108, 1994

Analysis of scintigrams by singular value decomposition (SVD) technique

Sauli E. SAVOLAINEN*,** and B. Kristian LIEWENDAHL*

*Department of Physics, University of Helsinki
**Department of Clinical Chemistry, Division of Nuclear Medicine, Helsinki University Central Hospital

The singular value decomposition (SVD) method is presented as a potential tool for analyzing gamma camera images. Mathematically image analysis is a study of matrixes as the standard scintigram is a digitized matrix presentation of the recorded photon fluence from radioactivity of the object. Each matrix element (pixel) consists of a number, which equals the detected counts of the object position. The analysis of images can be reduced to the analysis of the singular values of the matrix decomposition. In the present study the clinical usefulness of SVD was tested by analyzing two different kinds of scintigrams: brain images by single photon emission tomography (SPET), and liver and spleen planar images. It is concluded that SVD can be applied to the analysis of gamma camera images, and that it provides an objective method for interpretation of clinically relevant information contained in the images. In image filtering, SVD provides results comparable to conventional filtering. In addition, the study of singular values can be used for semiquantitation of radionuclide images as exemplified by brain SPET studies and liver-spleen planar studies.

Key words: brain, decomposition, factorization, filtering, spleen

INTRODUCTION

THE ISOTOPE IMAGE is a digitized presentation of the photon fluence impinging on the crystal from the radioactivity distribution of the object. The collected information consists of a large data matrix (usually 64×64 or 128×128) in which the signal and noise can be strongly connected to each other. Computing tools for data reduction (or filtering) are needed to offer the data in a more lucid form. Unitary transforms are used for the analysis of data matrixes.[1–4] In nuclear medicine imaging the objective is to detect organ uptake vs. blood or tissue background, or simply to identify uptake in the region of interest (ROI).

The analogy between the traditional frequency domain filter techniques and SVD spatial domain pseudoinverse filtering in the analysis of scintigrams has been shown by Raff et al.[5] Different forms of factor-analytical methods have been reported also for scintigram filtering.[6–8] In the analysis of dynamic gamma camera studies there are also various possibilities for the application of the principal components.[9–14]

In the present study the SVD method is presented as a potential tool for analysis and semiquantification of scintigrams. The clinical usefulness of SVD is demonstrated by the analysis of two different kinds of isotopic images: brain transversal single photon emission tomography (SPET) slices and planar spleen-liver region images.

MATERIALS AND METHODS

The transversal slices of brain perfusion SPET studies using Tc-99m-hexa-methyl-propyleneamine oxime (HM-PAO) were analyzed in seven subjects without apparent abnormalities and in four patients with the following diseases: herpes simplex virus encephalitis (HSVE), partial temporal epilepsy, dementia, and Sturge-Weber syndrome. As temporal lobe perfusion has been reported to vary with the phase of the HSVE disease[15] the SVD analysis was performed at various time intervals. Two clinically relevant SPET slices (each of 14 mm width) were included in each analysis.

A total of 86 static planar images (43 anterior and posterior) of the spleen and liver region in patients with

Received August 11, 1993, revision accepted December 6, 1993.

For reprint contact: Sauli Savolainen, Ph.D., Dept. of Physics, University of Helsinki, P.O. Box 9, FIN-00014 Helsinki, FINLAND.

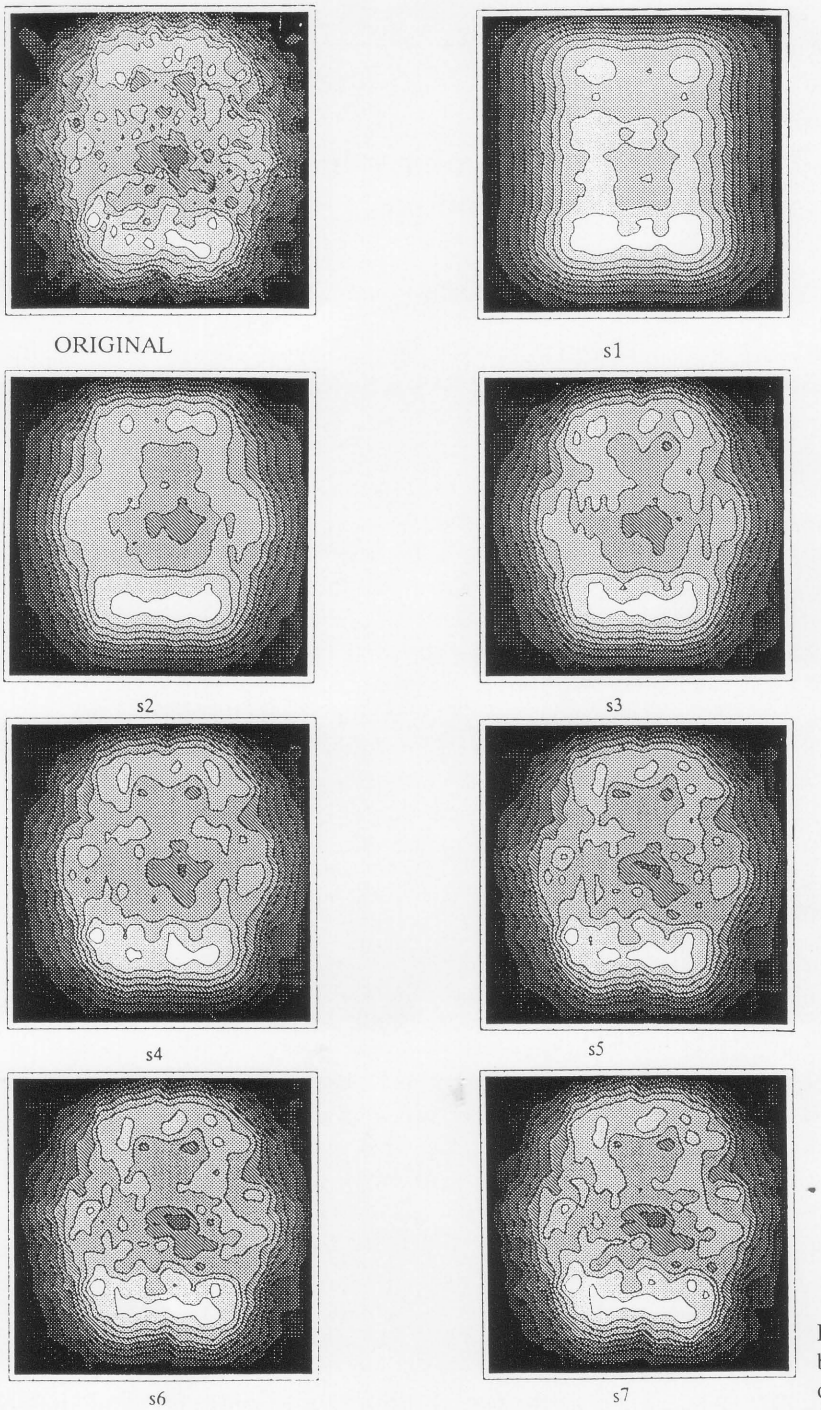

Fig. 1 Transversal slices of a normal SPET brain study reconstructed by varying numbers of singular values in decomposition (s1–s7).

idiopathic thrombocytopenic purpura (ITP) were analyzed after intravenous injection of ^{111}In-labelled platelets. Subsequent to posterior dynamic imaging anterior and posterior static imaging was performed at one hour as described previously.[16]

In both types of images the 64×64 matrix was divided into two matrices of 64×32, i.e. one including the spleen region and the other the liver region, and in brain studies one including the left and the other the right hemisphere of the brain. Therefore the analysis of images can be done by examining the singular vectors and corresponding s-values (see: Appendix 1).

RESULTS

Brain studies

In Figure 1 an original transversal slice and slices reconstructed with varying numbers of singular vectors of decomposition of a brain SPET study are presented. Figure 2 shows the side-to-side difference in temporal lobe radioactivity in a patient (Sturge-Weber syndrome) with a large hypoperfusion area in the right temporal lobe.

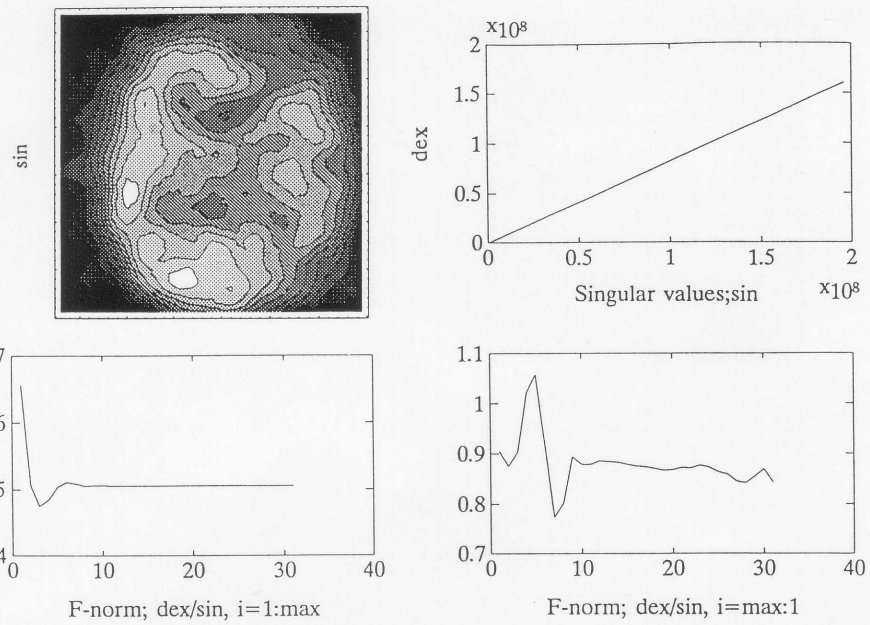

Fig. 2 An example of SVD analysis of SPET brain study in a patient with Sturge-Weber syndrome: a large hypoperfusion area in the right cerebral hemisphere can be seen. From upper left corner: contour of transversal slice, right (dex) vs. left (sin) singular values of corresponding matrixes, and the same expressed in the ratio of Frobenius norm (F-norm; vertical axis) by different index (i; horizontal axis) order: increasing (1 to maximum) and decreasing.

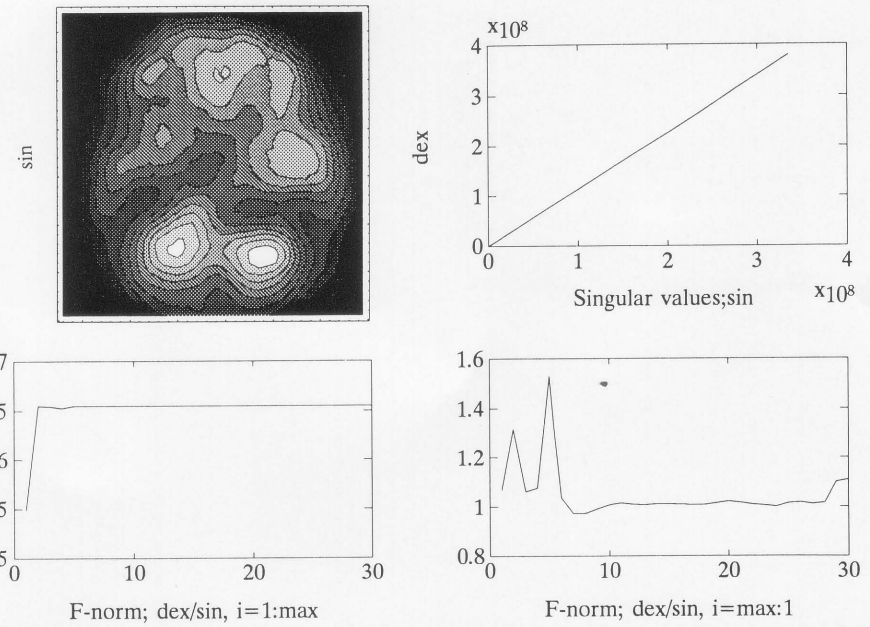

Fig. 3 SVD analysis of SPET brain study in a patient with epilepsy. A strong uptake of tracer in the right temporal lobe can be detected yielding a right-to-left ratio of 1.07 in F-norm.

The ratios of the singular values in the corresponding matrixes (64×32) are shown: the total right-to-left ratio in F-norm yields to the value 0.91. The same result can be observed whether the calculation is done either in increasing or decreasing order, i.e. the matrixes were compared so that the k first s-vectors (k takes on the values from 1 to 32) were taken into account and then the k last ones (from 32 to 1). The calculation shows that the difference is not only in "signal level", but also the "normal background" is significantly lower at the right side of the slice corresponding to a large change in brain perfusion.

The brain slice from a patient with an epileptic focus in the right temporal lobe is shown in Figure 3. The right-to-left ratio is 1.07 for the whole matrixes, but as can be seen in the lower right corner of the illustration the mean blood background yields to the ratio 1. There is a difference only

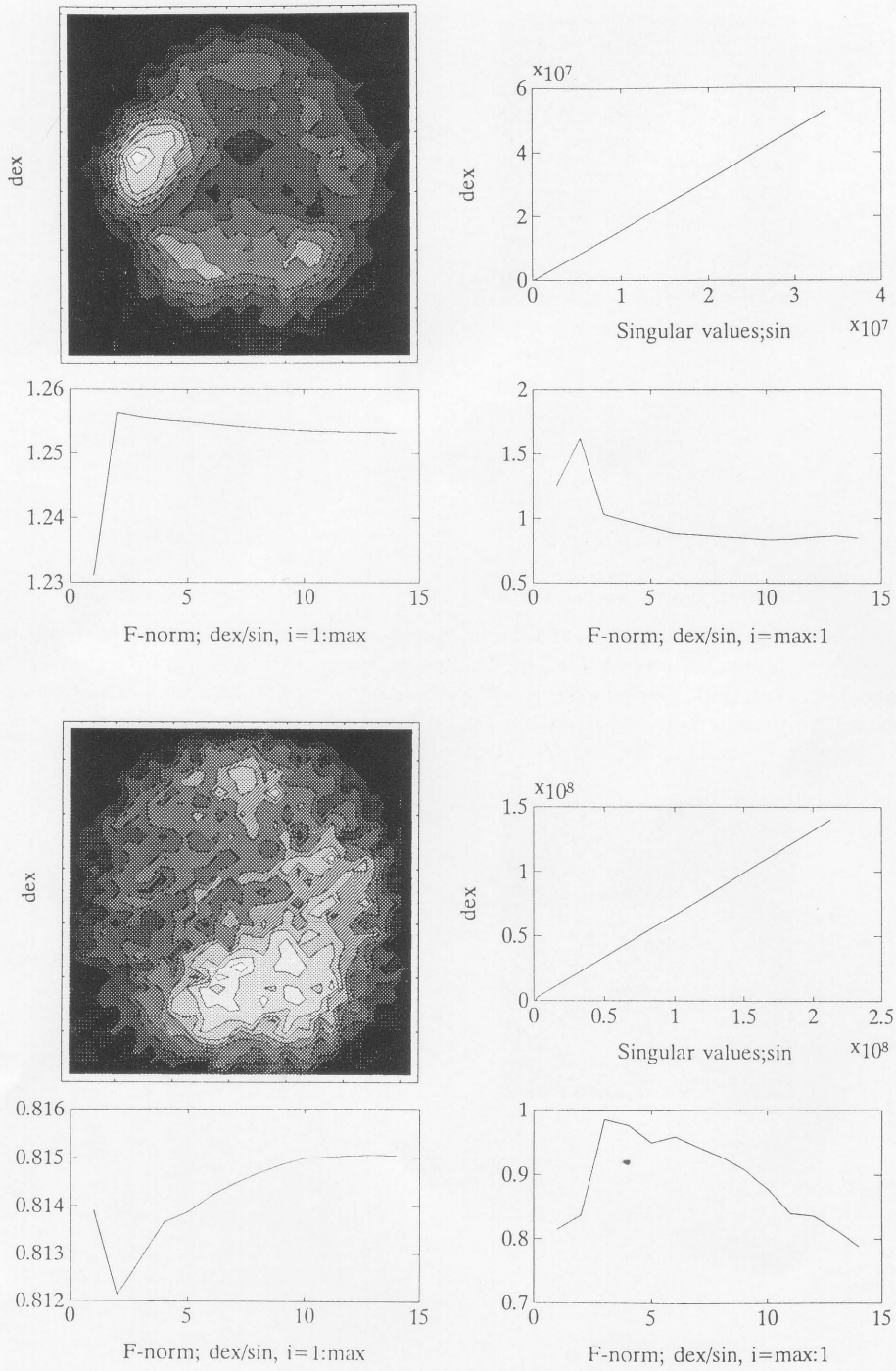

Fig. 4 SVD analysis of SPET brain study in a patient with acute phase HSVE (four upper figures) and during follow-up (four lower figures).

in the main singular values for the composition matrixes. Examples of side-to-side differences in the various phases of HSVE are shown in Figure 4. In the acute phase of the disease a strong hyperactive focus can be detected in the right temporal lobe yielding to a right-to-left ratio of 1.30. After three months the focus has disappeared and instead there is a hypoperfusion area in the region where the hyperactive focus was located. In the temporal lobes the right-to-left ratio is 0.81.

Side-to-side differences were also compared by "normalizing" the left and right matrixes by means of the whole slice matrixes. The F-norm of the S-matrix of the whole slice (64×64) formed with s-values with $C_k > 10$ were divided by the F-norm of S-matrixes of the right and left sides (64×32 each) formed with s-values with $C_k < 10$. The results are presented in Table 1. In normal subjects the mean side-to-side difference was $3.6 \pm 0.6\%$, and in patients with different diseases it varied form 6 to 30%.

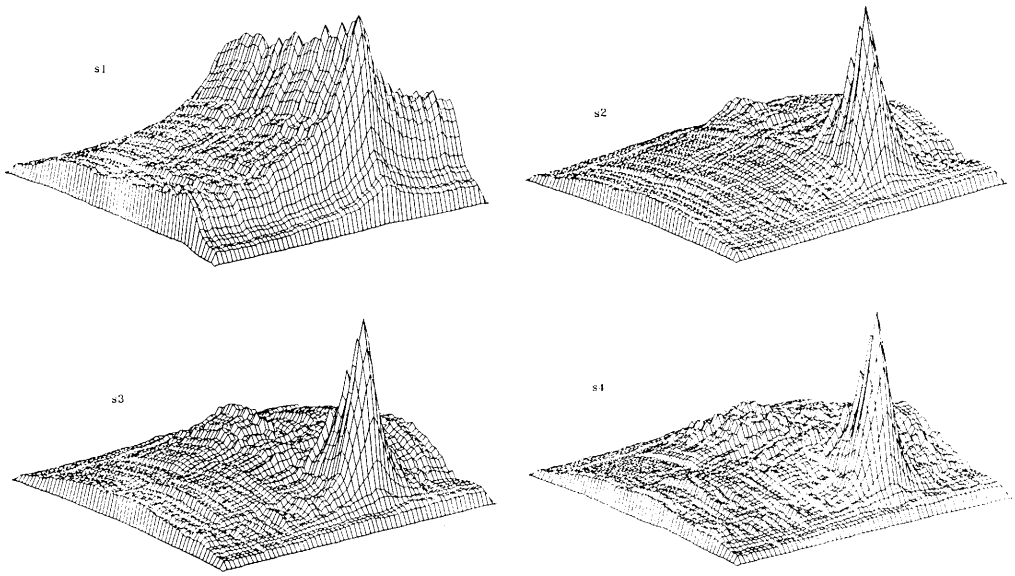

Fig. 5 SVD filtering of a activity distribution in the spleen-liver region (anterior view, 64 × 64 matrix, 3D-mesh presentation) one hour after injection of 3.7 MBq of In-111-labeled platelets. The image has been reconstructed by one, two, three, and four singular vectors.

Table 1 Side-to-side per cent differences in SPET brain slices in 7 normal subjects and in four patients with different diseases (each example consists of two slices, mean ± error is presented).

	right (%)	left (%)	difference (%)
Normal	13.9 ± 0.7	14.0 ± 0.6	3.6 ± 0.6
Dementia	12.9 ± 0.4	11.2 ± 0.3	14.5 ± 0.4
Epilepsy	14.0 ± 1.3	14.9 ± 1.4	6.6 ± 0.1
Sturge-Weber	13.7 ± 0.3	11.7 ± 0.1	20 ± 2
Acute HSVE*	15.7 ± 0.8	21.1 ± 1.1	29.2 ± 0.6
Late HSVE*	11.9 ± 0.1	11.0 ± 0.2	7.9 ± 1.4

*HSVE = herpes simplex virus encephalitis

Scintigrams of spleen-liver region

An example of a SVD filtered image is presented in Figure 5. The anterior image of the spleen-liver region reconstructed with 4 singular vectors forms a good approximation of the original image, but the background is reduced. The basis of the decomposition is shown in Figure 6. Vectors starting from 5 represent the noise rather than the signal in the image. The corresponding k for condition index (see: Appendix 1) $C_k < 10$ is 5 and for $C_k > 30$ is 22. The first 5 singular vectors are independent and thus can be considered as the basis of the signal, whereas the singular vectors from 22 to 64 essentially represent noise. The corresponding $E_{22} = 23\%$ indicates that the average noise (background) is 23% of the average spleen and liver uptake as calculated by means of matrix separation in F-norm.

The spleen-liver ratio calculated with singular values for the spleen and liver region matrixes was found to correlate with the values calculated by the conventional region of interest division method ($r = 0.85$, $p < 0.001$). The correlation is presented in Figure 7. Two 64 × 32 matrixes were analyzed in both anterior and posterior projections in all 43 cases, giving two sets of matrix decomposition: one for the spleen and one for the liver. The ratio was calculated in F-norm using the singular values which fulfil the requirement $C_k < 10$. The values are geometrical means of anterior and posterior values.[16]

DISCUSSION

The singular value decomposition has a wide variety of applications from solving linear least-square problems to data compression and SPET reconstruction.[17–21] The signal to noise ratio can be corrected by forming the image with those singular vectors which have the greatest impact in the decomposition used.[3,5–7] Image filtering is commonly performed in the frequency domain.[1,2,5] In conventional filtering the aim is to fix the frequency above a level where the signal can be considered to represent the background, while in SVD it is possible to decide which of the s-values belong to the object signal. There is therefore a frequency gap in both methods and it cannot be determined exactly whether these frequencies belong to the object signal or to the background. The optimum number of singular values in decomposition of brain SPET images seems to be from four to five as the various parts of the brain are well represented in these images. Optimal information on the spleen-liver region (Fig. 5) is obtained in reconstruction with four s-values. These results are in agreement with the results from phantom studies.[3,6,7] Noteworthy, the appropriate number of s-values depends on the matrix sizes and detected counts used.[5] For objec-

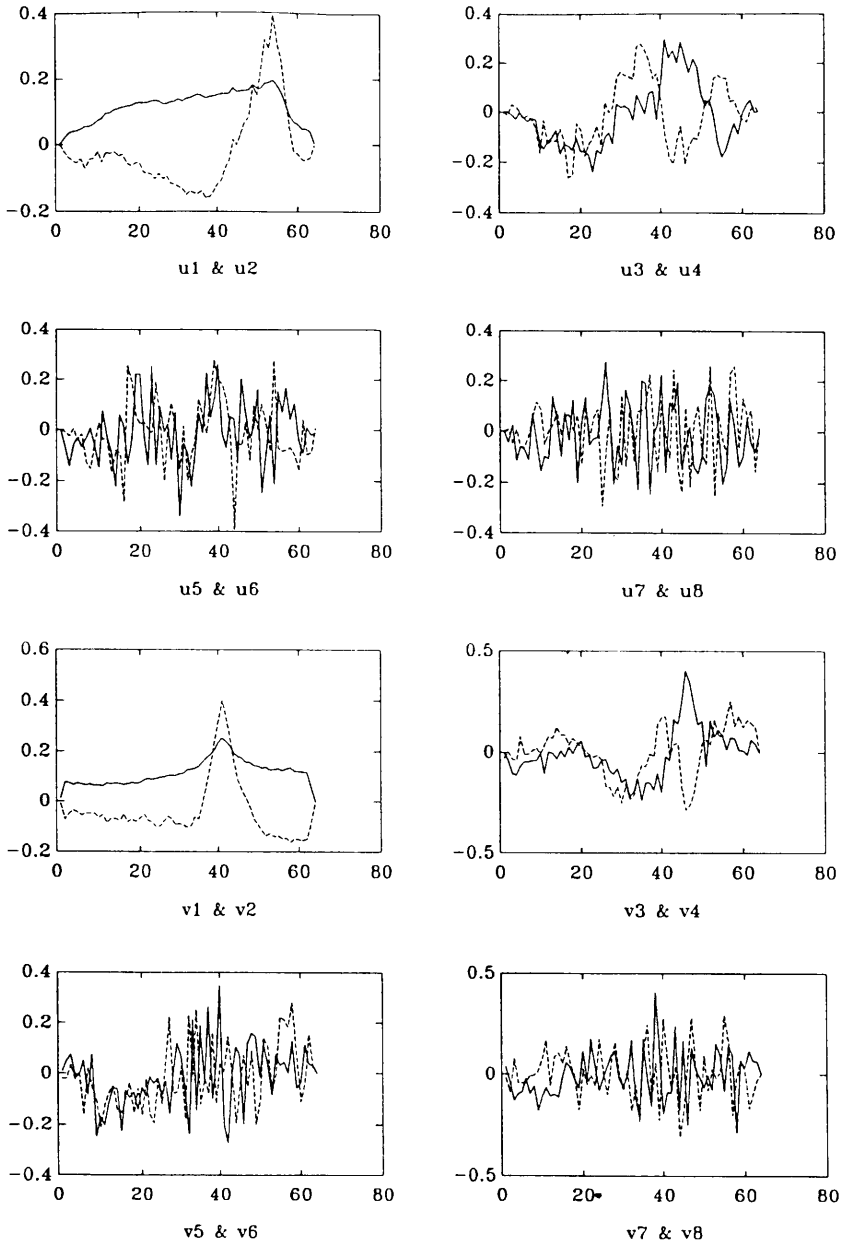

Fig. 6 The basis of the decomposition of the spleen-liver image shown in Fig. 5. As can be seen the basis vectors starting from six (in both directions; u and v, odd numbered vectors printed with continuous lines) do not seem to improve the information of the image as these vectors represent essentially background.

tive background correction in dynamic scintigraphic studies more comprehensive factoring methods will be needed.[22]

In nuclear medicine identification of tracer uptake is usually achieved by comparing activities in regions of interest (ROIs), but there may be problems in determining ROIs when the signal to noise ratio is low. The advantage of the SVD analysis is that it is fully user independent, i.e. ROIs chosen or background selected do not cause artefacts. In addition, the SVD analysis gives new information on the images studied. It has been observed that the level of platelet autoantibodies in the blood influences platelet dynamics in ITP patients.[16,23] In this study E_k and C_k were found to be associated with the level of circulating antibodies. The patients, all studied with autologous platelets, were divided into three subgroups as described previously[16,23]: no (= 0), small (= 1), and large (= 2) concentration of antibodies in the blood. E_2 and E_{10} were significantly higher (in t-test) in patient group 0 than in 1 or 2 (E_2 [%]: 0 vs. 1, 38 to 32, p = 0.008, 0 vs. 2, 38 to 33, p = 0.014; E_{10} [%]: 0 vs. 1, 23 to 20, p = 0.04) indicating that the blood background is higher in patients with no antibodies than in patients with antibodies. Also the quotients C_k (see: Appendix 1) indicate that the blood

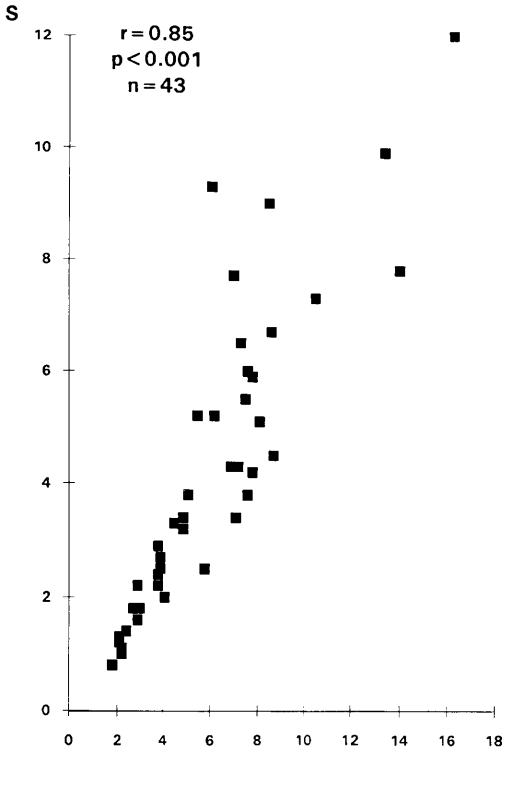

Fig. 7 The calculated spleen-liver ratios based on the main singular values of the corresponding matrixes (S) correlated with the conventional region-of-interest division method (R).

background and the signal are somewhat dependent on each other in patients with no antibodies compared to cases with antibodies.

The spleen-liver ratio has clinical relevance in ITP and several other diseases but the methods used for the determination of this ratio have varied greatly.[16,23–26] The method used here is a mathematical one and does not take into account scatter or attenuation of radiation in the images. The results shown in Table 1 are an attempt to normalize a single brain study so that it would not be necessary to compare each case with normal data in order to decide whether there is hypoperfusion or hyperperfusion. The idea is to compare the main singular values for the right and left matrixes to the "normal background" in each slice by calculating the separation of those matrixes which could explain this phenomenon. However, in a very abnormal situation (side-to-side difference > 30%) the method does not seem to be suitable; the higher the main s-value the smaller the lowest s-value. Thus, a very strong focus will give a too low "background" and thus misestimate the real difference.

The examples from nuclear medicine studies presented in this paper show that SVD can be used for filtering. However, any kind of filtering of original data will destroy some information: the cut-off frequency in frequency filtering and the number of significant components in decomposition are similarly non-unique. To provide the physiological meaning of the s-components can be difficult, but a clinical explanation for the "factors" can be provided as exemplified in the present study. It is concluded that SVD is a potentially clinically useful mathematical tool for the analysis and semiquantitation of scintigrams as it can be considered an objective method for the interpretation of data contained in the scintigram.

ACKNOWLEDGMENTS

This work was supported by a grant from the Finnish Society of Nuclear Medicine.

REFERENCES

1. Pratt WK. *Digital Image Processing.* New York: Wiley & Sons, pp. 376–382, 1991.
2. Gonzales RC, Wintz P. *Digital Image Processing.* Massachusetts: Addison-Wesley, pp. 61–135, 213–251, 1987.
3. Morf R, Roesel F, Schmidlin P. Pattern recognition in noisy pictures. *Research report (RZ 778, 26491, 8/13/76) by IBM Research Division.* Yorktown Heights, New York, pp. 1–17, 1976.
4. Golub GH, van Loan CF. *Matrix computations.* Baltimore: The Johns Hopkins University Press, 1989.
5. Raff U, Stroud DN, Hendee WR. Improvement of lesion detection in scintigraphic images by SVD techniques for resolution recovery. *IEEE Trans Med Imaging* 5: 35–44, 1986.
6. di Paola R, Berche C, Bazin JP: Traitement digital des informations scintigraphiques. *In* Nuklearmedizin: Proceedings of 12th annual meeting of the Society of Nuclear Medicine-Europe, München, September 11.–14., 1974. Pabst HW et al. (ed.). Stuttgart: F.K. Schattauer Verlag GmbH, pp. 670–683, 1975.
7. Schmidlin P, Schlegel W, Rösel F. Qualitätskriterien der Faktoranalytischen Bildbearbeitung in der Szintigraphie. *In* Nuklearmedizin: Proceedings of 13th annual meeting of the Society of Nuclear Medicine-Europe, Copenhagen, September 10–13, 1975. Munkner T et al. (ed.). Stuttgart: F.K. Schattauer Verlag GmbH, pp. 80–93, 1977.
8. Savolainen S, Liewendahl K. Use of singular value decomposition for interpretation of gamma images. *In* Nuclear Medicine. Nuclear medicine in research and practice. Proceedings of European nuclear medicine congress 1991, Vienna, September 1.–5., 1991. Schmidt HAE and Höfer R (eds.). Schattauer Stuttgart-New York, XXXVIII-XLII, 1992.
9. Schmidlin P, Clorius J, Kubesch R, et al. Evaluation of dynamic studies by means of factor analysis. *In* Medical radionuclide imaging, Vienna: International Atomic Energy Agency (IAEA-SM-210/27), pp. 397–408, 1977.
10. Schmidlin P. Quantitative evaluation and imaging of functions using pattern recognition methods. *Phys Med Biol* 24: 385–395, 1979.
11. Barber DC. The use of principal components in the quantitative analysis of gamma camera dynamics studies. *Phys Med Biol* 25: 283–292, 1980.
12. Oppenheim BE, Appledorn CR. Functional renal imaging

through factor analysis. J *Nucl Med* 22: 417–423, 1981.
13. Cavailloles F, Bazin J-P, di Paola R. Factor analysis in gated cardiac studies. J *Nucl Med* 25: 1067–1079, 1984.
14. Ito T, Maeda H, Takeda K, et al. Factor analysis of gated cardiac blood-pool data: application to patients with congenital heart disease. *Nucl Med Commun* 12: 865–873, 1991.
15. Launes J, Nikkinen P, Lindroth L, et al. Diagnosis of acute herpes simplex encephalitis by brain perfusion single photon emission computed tomography. *Lancet* 1: 1188–1191, 1988.
16. Savolainen S, Liewendahl K, Syrjälä MT, et al. Platelet splenic transit times in idiopathic thrombocytopenic purpura, Compartmental vs. non-compartmental model. *Int J Hematol* 55: 81–87, 1992.
17. Belsley DA, Kuh E, Welsch RE. *Regression diagnostics: Identifying influential data and source of collinearity.* New York: Wiley & Sons, pp. 98–191, 1980.
18. Muzik O, Herzoc KJ, Langen E, et al. *In vivo* assay of blood-brain-barrier function regarding glucose transport using ^{11}CMG and PET. *In* Positron emission tomography in clinical research and clinical diagnosis: tracer modelling and radioreceptors, Beckers et al. (ed.). London: Kluwer academic publisher, pp. 194–205, 1989.
19. Kahaner D, Moler C, Nash S. *Numerical methods and software.* New Jersey: Prentice-Hall International Editions, pp. 218–226, 1989.
20. Umeyama S. Least-squares estimation of transformation parameters between two point patterns. *IEEE Trans Pattern Anal Machine Intell* 4: 376–380, 1991.
21. Smith MF, Floyd CE, Jaszczak RJ, et al. Reconstruction of SPECT images using generalized matrix inverses. *IEEE Trans Med Imaging* 11: 165–175, 1992.
22. Van Daele M, Joosten J, Devos P, et al. Background correction in factor analysis of dynamic scintigraphy studies: necessity and implementation. *Phys Med Biol* 35: 1477–1485, 1990.
23. Savolainen S. Spect versus planar scintigraphy for quantitation of splenic sequestration of ^{111}In-labelled platelets. *Nucl Med Commun* 13: 757–763, 1992.
24. Chandler ST. A comparison of liver-spleen ratios and uptakes obtained using planar and tomographic techniques. *Nucl Med Commun* 10: 297–307, 1989.
25. Reenen van, Lötter MG, Heyns A duP, et al. Quantification of the distribution of ^{111}In-labelled platelets in organs. *Eur J Nucl Med* 7: 80–84, 1982.
26. Rensburg van AJ, Lotter MG, Heyns A duP, et al. An evaluation of four methods of ^{111}In planar image qualification. *Med Phys* 15: 853–861, 1988.
27. Dongarra JJ, Moler CB, Bunch JR, et al. *Linpack users' guide.* Philadelphia: SIAM, 1979.

APPENDIX 1

Any $n \times m$ matrix **A** of rank r ($r < m < n$) can be expressed in the form[4]:

$$\mathbf{A} = \mathbf{USV}^T \tag{1}$$

where **U** is an $n \times m$ matrix with columns consisting of m orthogonal unit eigenvectors associated with the m largest eigenvalues of $\mathbf{AA}^T$, **V** is an $m \times m$ orthogonal matrix consisting of the orthogonal unit eigenvectors of the $m \times m$ matrix $\mathbf{A}^T\mathbf{A}$, and **S** a diagonal $m \times m$ matrix, whose elements (s_i) are non-negative and in decreasing order. The elements of **S** are the singular values of matrix **A**, *i.e.* they are the square roots of eigenvalues of matrix $\mathbf{A}^T\mathbf{A}$. The presentation of matrix **A** in the form (1) is called the Singular Value Decomposition (SVD). An element a_{ij} of **A** can be expressed as follows:

$$a_{ij} = \sum_{k=1}^{r} s_k u_{ik} v_{jk} \tag{2}$$

The algorithm for SVD was described by Dongarra et al.[27]

The singular vectors **U** form an orthonormal basis for the matrix **A**. If all the singular vectors are used as the basis of matrix **A** (i.e. image) the decomposition will give the exact presentation of the original matrix **A**. If only k first is used, the image will be an approximation of the original one. The elements of **S** indicate the significance of vectors $\mathbf{u}_i$ in the decomposition. The condition index (C_k) of each singular value (s-value) is the quotient between the highest and the current s-value[4]:

$$C_k = s_1/s_k \tag{3}$$

If the quotient is low (< 10), then no dependency between corresponding vectors exists but if this quotient is high (> 30) then there is a serious dependency between the parameters.[4,17,18] Another possibility to estimate the significance of vectors $\mathbf{u}_i$ in the decomposition is to calculate the separation between the original and the matrix formed by using only the first k s-vectors in decomposition.[4] The separation can be called Error Level E_k:

$$E_k = 100\% \times \frac{|A - A'|_F}{|A|_F} = \sqrt{\frac{\sum_{i=k+1}^{n} S_i^2}{\sum_{i=1}^{n} S_i^2}} \times 100\% \tag{4}$$

where the approximate matrix $\mathbf{A}'$ is formed by using only the first k s-values (F refers to Frobenius norm: F-norm). The smaller the E_k, the better the first k singular vectors $\mathbf{u}_i$ represents the original image. Thus, C_k gives the answer to how many eigenvectors form the signal, which is independent of the other components of the matrix. E_k can be considered as a measure of the noise, which is related to the blood background of the object. In clinically comparable images the statistical (white) noise as well as noise due to the scatter can be considered equal. Therefore, possible significant changes in the background level must be related to the different background activities of surrounding tissues.